euronoise

Multipath reflection from surface waves

Chris Tindle[a], Grant Deane[b] and James Preisig[c]

[a]Physics Department, University of Auckland, Bag 92019, 1010 Auckland, New Zealand
[b]Scripps Inst. Oceanography, Univ. Califiornia, San Diego, La Jolla, CA 92093, USA
[c]Woods Hole Oceanographic Institution, Bigelow 404, MS#9, Woods Hole, MA 02543, USA
c.tindle@auckland.ac.nz

A tank experiment was conducted at Scripps Institution of Oceanography to measure reflection of underwater sound from surface waves. Short pulses at a nominal 200 kHz were transmitted beneath surface waves of wavelength 0.7 m to a receiver at 1.2 m range. The surface wave crests act as curved mirrors for underwater sound and lead to focussing and caustics in the surface reflected pulses. The locations of the foci and caustics move steadily as the wave progresses and lead to rapid variation of amplitude, phase and arrival time of the received pulses. Wavefront modelling has been used to calculate theoretical waveforms for the measured surface wave shape. The theory shows there are typically three distinct reflected eigenrays beneath a wave crest and they interfere to give rapid variation of the received signal. The theory gives good agreement with the details of the time dependent interference of the surface reflected pulses. [Work supported by ONR]

1 The Experiment

A sketch of the experimental arrangement is shown in Fig. 1. Travelling waves at 1.5 Hz were generated in a wave tank by a paddle at one end. The waves were absorbed at the other end so there were no reflected waves.

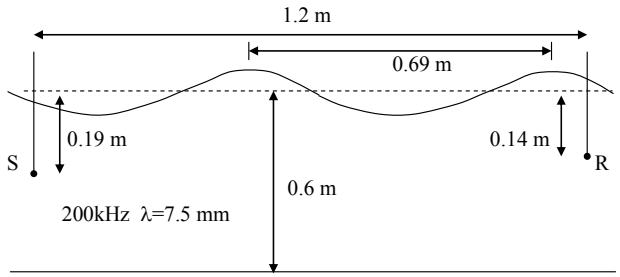

Fig. 1 Experimental arrangement

A source S at a nominal 200 kHz and wavelength 7.5 mm emitted a smoothed two-cycle pulse. The receiver R was positioned so that the direct and surface reflected pulses were received before any reflections from the walls or the bottom. It was necessary to allow reverberation to decay away between pulses but a transmission rate of 180 pulses per second was achieved and this gave 120 pulses per surface wave cycle.

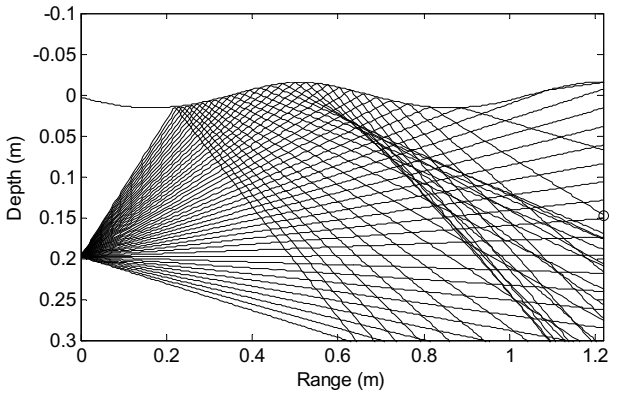

Fig. 2 Ray trace for ping 31.

Figure 2 shows a ray trace for one particular position of the surface wave. The crest at 0.5 m range acts like a curved mirror for sound and the rays focus at 0.61 m range. After passing through the focus the rays diverge and fan out to give a region bounded above and below by a caustic. The receiver position is marked by the small circle on the right of the figure. For the situation shown, the receiver has a direct eigenray and one surface reflected eigenray. As the wave progresses the fan of rays bounded by the caustic sweeps up over the receiver. When the receiver is between the caustics it receives three surface reflected eigenrays as will be discussed in detail below.

2 Wavefront modelling

Wavefront modelling is a method of finding receiver waveforms for pulse propagation in shallow water and was described in Ref. 1. The method is able to handle the rapid range dependence associated with reflection of pulses from surface waves.

Wavefront modelling is a direct solution of the wave equation and expresses the field as a sum of terms, each of which is a phase integral. The pressure p_{nj} at range r and depth z for a given sequence of reflections can be written

$$p_{nj}(r,z) = Q(2\pi r)^{-1/2} e^{i\pi/4} \int_{-\infty}^{\infty} [(\omega/c_s)\cos\theta_s]^{1/2} \times \prod_{1}^{n_j'} |R_a| \prod_{1}^{n_j''} |R_b| \exp(i\phi_{nj}+\delta_0) (d\theta_r/d\theta_s)^{1/2} d\theta_s \qquad (1)$$

where Q is the source strength, ω is the angular frequency, c_s is the sound speed at the source, θ_s and θ_r are ray angles at source and receiver, R_a and R_b are reflection coefficients at upper and lower turning points, and n_j' and n_j'' are the number of upper and lower reflections.

The phase ϕ_{nj} corresponds to the accumulated phase along a ray path and is given by

$$\phi_{nj} = \int_{z_s\sim}^{z} (\omega/c)\sin\theta \, dz' + \sum_{1}^{n_j'} \psi_a + \sum_{1}^{n_j''} \psi_b + \int_{0}^{r} (\omega/c)\cos\theta \, dr \qquad (2)$$

where θ is the changing ray angle along the path, and ψ_a and ψ_b are the phase changes at each reflection. The notation $z_s\sim$ means that the integral follows the ray path up and down and successive sections are summed.

The parameter δ_0 is a residual phase arising from square root terms.

$$\delta_0 = (\pi/4)[1 - \text{signum}(\theta_s\theta_r)] \qquad (3)$$

The phase integral can be evaluated approximately using its behaviour near points of stationary phase as described in detail in Refs. 1 and 2. For an isolated ray there is a single point of stationary phase and the result can be written

$$p_{nj} = Qr^{-1/2} \prod_{1}^{n_j'} |R_a| \prod_{1}^{n_j''} |R_b| \, [(\omega/c_s)\cos\theta_s]^{1/2} \times [(\omega/c_r)\cos\theta_r]^{-1/2} |dz^*/d\theta_s|^{-1/2} \exp[i(\phi_{nj}+\delta)] \qquad (4)$$

where z* is the depth at the receiver range of the ray with launch angle θ_s and δ is given by

$$\delta = (\pi/4)\,[1 - \text{signum}(\theta_s\theta_r dz^*/d\theta_s)] \qquad (5)$$

The expression for the pressure in Eq. (4) is identical to that deduced from ray geometry and energy conservation.

In the vicinity of a caustic there are two nearby points of stationary phase which must be treated as a pair using an Airy function. The result can be written

$$p_{nj} = Q(2\pi/r)^{1/2} e^{i\pi/4} \prod_{1}^{n_j'} |R_a| \prod_{1}^{n_j''} |R_b| [(\omega/c_s)\cos\theta_s]^{1/2}$$

$$\times |d\theta_r/d\theta_s|^{1/2}\, \beta\, \exp[i(\phi_0+\delta_0)]\, \text{Ai}(-|\phi_0'\beta|) \qquad (6)$$

where

$$\beta = |\phi_0'''/2|^{-1/3} \qquad (7)$$

The field given by Eq. (6) is finite on the caustic and decays steadily into the shadow zone. The derivatives ϕ_0' and ϕ_0''' are found numerically from the ray trace as described in Ref. 1. The Airy function expression must be used when the phase difference of the pair is less than $\pi/2$.

In the vicinity of a focus there are three nearby points of stationary phase which are treated together using a Pearcey function. The result can be written

$$p_{nj} = Q(2\pi r)^{-1/2} e^{i\pi/4} \prod_{1}^{n_j'} |R_a| \prod_{1}^{n_j''} |R_b| [(\omega/c_s)\cos\theta_s]^{1/2}$$

$$\times |d\theta_r/d\theta_s|^{1/2}\, \alpha\, \exp[i(\phi_0+\delta_0)]\, \text{Pc}(\alpha\phi_0', \alpha^2\phi_0''/2) \qquad (8)$$

where

$$\alpha = (\phi_0''''/24)^{-1/4} \qquad (9)$$

The field given by Eq. (8) is finite at the focus and joins smoothly to the Airy function expressions for the caustics. The Pearcey function must be used when the phase differences of the three rays are less than $\pi/2$.

In each application the parameters for the Airy and Pearcey functions are determined numerically from the phase function obtained from the travel time along the ray path. This procedure gives the amplitude, phase and travel time for each contribution to the acoustic field at the receiver. The received waveform can then be constructed by combining pulses of the correct amplitude, phase and arrival time for each contribution.

Results

A series of experimental run were made with surface waves of different heights. Representative results for Run 104 are shown in Figs. 2 and 3. The wave height is 31 mm or 4.1 acoustic wavelengths. There were 120 pings in each surface wave cycle. Eigenrays and waveforms for selected pings are shown.

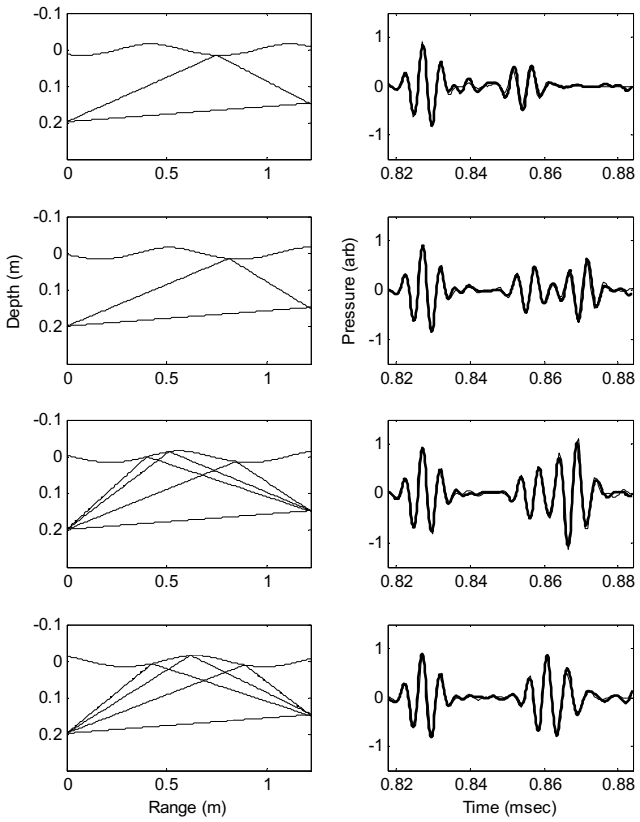

Fig. 3 Run 104, pings 15, 31, 40, 53. The left panels show eigenrays. The right panels show receiver waveforms (data thick line, model thin line).

The left panels in Figs. 3 and 4 show the eigenrays for successive positions of the surface wave. The right panels show the experimental waveforms as thick lines and the waveforms calculated using the wavefront model as thin lines. In all cases the first pulse in the waveforms is from the direct ray and does not change as the surface wave moves. The second pulse in the waveform shows interference structure from up to three surface reflected ray paths.

The top panels in Fig. 3 have the wave crest at 0.4 m range. There is one surface reflected eigenray and the waveforms show two simple arrivals.

The second panels in Fig. 3 have the wave crest at 0.5 m range. The ray trace for this situation was shown in Fig. 2 which shows that the receiver is just above the upper caustic. The corresponding panels in Fig. 3 show that there is only one surface reflected eigenray but the waveform apparently shows two surface reflected pulses. The second pulse is due to the diffraction of energy into the shadow zone of the upper caustic of Fig. 2. The third panels of Fig. 4 are similar. There is only one eigenray but two surface reflected pulses. The lower caustic has moved above the receiver and the energy diffracts into the shadow zone to give a second surface reflected pulse.

In the lower two panels of Fig. 3 and the upper two panels of Fig. 4 there are three surface reflected eigenrays which combine to give complicated waveforms.

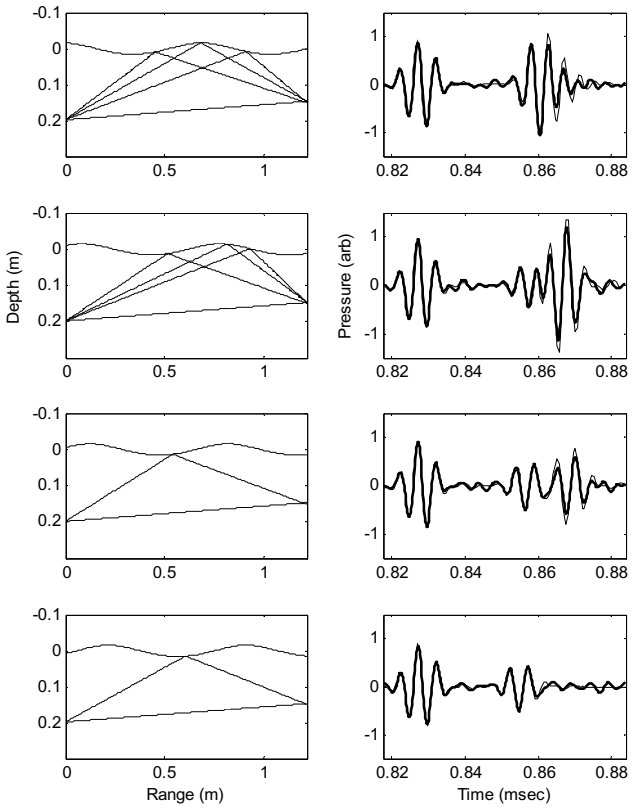

Fig. 4 Run 104, pings 61, 77, 84, 100. The left panels show eigenrays. The right panels show receiver waveforms (data thick line, model thin line).

A movie of the results for Run 104 and for other wave heights can be seen on the web site

http://www.phy.auckland.ac.nz/html/c_tindle.html.

3 Conclusions

In all cases in Figs. 3 and 4 the wavefront model gives waveforms in good agreement with the experimental waveforms. This verifies the model and justifies the ray trace and drawing of eigenrays. The results also show that a ray model is not just a high frequency approximation. In fact, this is a low frequency situation because the interfering ray paths differ by only a few wavelengths and lead to strong overlap of the pulses.

The strong amplitude and phase changes associated with reflection of underwater sound from surface waves have important consequences for the design of underwater communications systems. The present results show that the process can be successfully modelled and that the detailed interference of the different ray paths is well understood.

Acknowledgments

The support of the Office of Naval Research, Grant No. N00014-04-1-0728 is gratefully acknowledged.

References

[1] C. T. Tindle and G. B. Deane, "Shallow water sound propagation with surface waves," J. Acoust. Soc. Am. **117**, 2783-2794 (2005).

[2] C. T. Tindle, "Wavefronts and waveforms in deep-water sound propagation," J. Acoust. Soc. Am. **112**, 464-475 ((2002).